Use of High-Resolution Multispectral Imagery to Assess the Role of Sand and Gravel Shoals for Flood-Infrastructure Interaction in the Yellowstone River, Montana

Fred Falcone Jr.[1]; Nina Stark, Ph.D., M.ASCE[2]; Michael Gardner, Ph.D., P.E., M.ASCE[3]; Anne Lemnitzer, Ph.D., M.ASCE[4]; Nicola Brilli, Ph.D.[5]; Rodrigo Sarlo, Ph.D.[6]; Jonathan Hubler, Ph.D., A.M.ASCE[7]; and Mohammad Khosravi, Ph.D., M.ASCE[8]

[1]Charles E. Via, Jr. Dept. of Civil and Environmental Engineering, Virginia Tech, Blacksburg, VA (corresponding author). Email: ftf4250@vt.edu
[2]Engineering School for Sustainable Infrastructure and Environment, Univ. of Florida, Gainesville, FL; formerly, Charles E. Via, Jr. Dept. of Civil and Environmental Engineering, Virginia Polytechnic Institute and State Univ., Blacksburg, VA
[3]Dept. of Civil and Environmental Engineering, Univ. of California, Davis, Davis, CA; formerly, Dept. of Geological Sciences and Engineering, Univ. of Nevada, Reno, NV
[4]Samueli School of Engineering, Univ. of California, Irvine, Irvine, CA; Villanova Univ., Villanova, PA
[5]Charles E. Via, Jr. Dept. of Civil and Environmental Engineering, Virginia Tech, Blacksburg, VA
[6]Charles E. Via, Jr. Dept. of Civil and Environmental Engineering, Virginia Tech, Blacksburg, VA
[7]Dept. of Civil and Environmental Engineering, Villanova Univ., Villanova, PA
[8]Dept. of Civil Engineering, Montana State Univ., Bozeman, MT

ABSTRACT

Gravel and sand shoals may play a significant role for infrastructure impacts during flood events. This study uses high-resolution (30-cm panchromatic resolution at nadir) pan sharpened multispectral satellite images to map sand and gravel shoals near the Cinnabar Basin Bridge in Gardiner, Montana. While the bridge was not damaged during the flood event, erosion of the riverbanks and scour were observed with significant differences noticeable between both riverbanks, which may be related to the presence or evolution of shoals during the flooding. Toward analyzing the role of the shoals on local erosion and scour patterns, the goal of this study is to classify sediments based on soil type (sand, gravel, and cobbles) and color, using unsupervised K-means clustering and spectral information divergence (SID) with images taken in October 2022 and January 2023. The soil classifications from the K-means clustering and SID analysis are then compared to the pan sharped RGB images, drone images, and on-site observations and photos to assess the results from the classifications. The resulting classifications are compared for changes in the composition of the shoals over time from the October image to the January image, but also take advantage of receding water levels over the winter. Both the K-means clustering and SID analysis yield sediment classifications matching the site photos and drone images. Results show that unsupervised K-means clustering and SID can be used to classify sediments into different groups based on soil type and color, which may enable a deeper investigation of the impacts of sand and gravel shoals on infrastructure.

INTRODUCTION

The study area is the Yellowstone River around the Cinnabar Basin Road Bridge in Gardiner Montana. This section of the Yellowstone River is a relatively straight with gravel, cobble, and

sand shoals upstream and downstream of the bridge. The pansharpened TrueColor images of the site are presented in Figure 1. In the images, the downstream shoal is at the top and the upstream shoal is at the bottom. Based on onsite observations of the eroded banks, the riverbanks in the area generally consist of sand and gravel. The Geotechnical Extreme Event Reconnaissance (GEER) association conducted field reconnaissance missions to the site in July 2022 and October 2022 after the record flooding that occurred in June 2022. Data collected during the reconnaissance relevant to this study include site photos, multispectral drone imagery, sediment sampling and characterization.

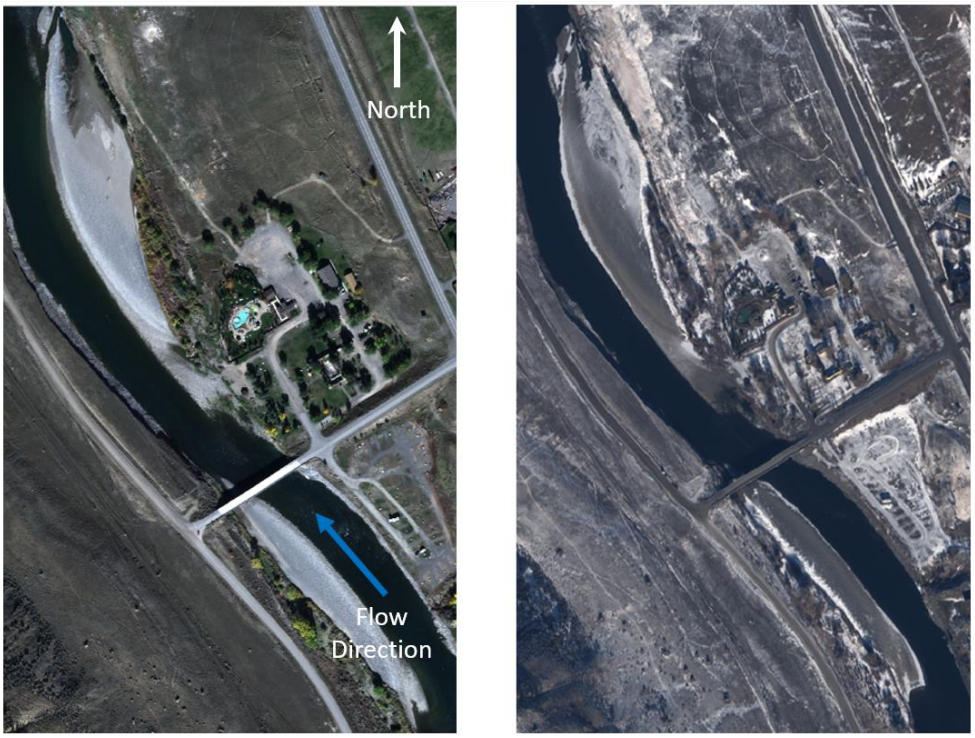

Figure 1. Pansharpened (30cm pixels) TrueColor image of the Cinnabar Basin Bridge (N45° 6' 41.5476", W110° 47' 34.9872"), Gardiner Montana, collected on October 18, 2022 (left) and January 4, 2023 (right). Downstream is toward the top of the images. Pléiades-Neo Product © COPYRIGHT AIRBUS DS, France, all rights reserved.

The shoals upstream and downstream of the bridge narrow the river. While the downstream shoal has no effect on the bridge, the narrowing upstream of the bridge can cause an increase in water velocity and redirection of flow, which can lead to constriction scour in the river channel around the bridge piers and increased bridge pier scour (Sumer and Fredsøe 2022, FHWA 2005). Tracking the composition and geomorphology of the shoals with remote sensing may allow more insight on how shoal geomorphodynamics may affect infrastructure with time. Also, gravel and cobble shoals are likely less erodible than sandy-gravelly riverbanks, possibly leading to an increased riverbank erosion in the presence of the coarse-grained shoals.

To complement the field data acquired during the July and October 2022 site visits two satellite images from the Pléiades-Neo satellite constellation were acquired, one from October 18, 2022, shortly after the second field survey, and one from January 4, 2023. The goal of the

satellite images was to classify the soil types in the shoals upstream and downstream of the bridge and to evaluate changes overtime between the two images and related to lower water levels. The Pléiades-Neo satellite constellation uses a very high-resolution multispectral instrument. It captures images in 6 multispectral bands, red (RED) (619-690nm), green (GREEN) (533-591nm), blue (446-520nm), red edge (697-750nm), near infrared (NIR) (769-888nm), and deep blue (416-457nm), with spatial resolutions of 1.2m at nadir, and a panchromatic band (460-818nm) with a spatial resolution of 0.3m at nadir (Airbus 2021). This high resolution is expected to enable mapping of variations of soils type as well as riverbanks on relevant scale to assess infrastructure impacts.

Previous studies have shown that satellite images can be used to classify soils, creek beds, and vegetation (Lecki et al. 2005, Wolf 2012, Ahmed et al, 2014, Stark et al. 2019). The study by Lecki et al. (2005) showed that multispectral images could be used to classify water, sediments, and vegetation in a stream bed. Stark et al. (2019) showed that multispectral satellite images can successfully provide a simplified sediment classification for coastal sediments based on knowledge of sediment color and local geology. The objective of the study is to outline a method to produce high resolution soil classification maps for sand and gravel shoals using high resolution multispectral imagery.

METHODS

The Pléiades-Neo multispectral images (1.2m spatial resolution at Nadir) were pansharpened to a spatial resolution of 0.3m using the panchromatic bands from the images. Each of the multispectral bands were pansharpened in QGIS software using the cubic resampling method. The cubic resampling method provides sharp images with minimal geometric distortion, however, has the possibility of pixel values exceeding the input values (ERDAS 2005). It has been shown that the cubic resampling method for raster data can lead to less error than other methods such as nearest neighbor, and bilinear (Smith et. al 2004). For these reasons the cubic resampling method was selected for the analysis. The pansharpening step increases the resolution of the multispectral bands to the resolution of the panchromatic band, which increases the number of pixels in each band by a factor of 16 for the Pléiades-Neo images. Using this method greatly increases the detail of the images and analysis results.

The pansharpened multispectral bands were corrected to Top of Atmosphere (TOA) Reflectance using the correction factors provided in the satellite image metadata and the equations provided by the Pléiades User Manual (Airbus 2021). While this step is not explicitly required for the analysis, it helps create a more uniform data set when comparing images from two different days with different illumination conditions, as it normalizes the reflectance values for differences in sun position and distances from earth. Reflectance values were not corrected for atmospheric conditions. Atmospheric conditions are not expected to impact the results because external reference spectra were not used for the analysis.

The images were classified using two methods, K-Means Clustering, and Spectral Information Divergence (SID). K-Means clustering is an iterative clustering algorithm where pixel values in an image are grouped in a specified number of clusters based on the pixel value, distance from the cluster centroid, and variance from the average value of pixels in the cluster (Hartigan and Wong 1979). This method allows similar pixels to be grouped together (such as pixels that represent gravel or sand); however, it can only be used with one spectral band at a time and will yield different results for each band, because different materials have different

reflectance values in each band. For this analysis the red band was selected for the K-means clustering because it had the largest range of reflectance values in the shoals. The number of iterations was limited to ten for the analysis. Beyond ten iterations there was no notable increase in classification of the shoals but an increase in processing time.

SID is a spectral classification method that clusters pixels by using the divergence of pixels across all bands to match them to a reference spectrum. The less divergence between the pixels the more likely the pixels are similar (i.e., a similar material like sand or gravel) (Baodong et al. 2008). In this case, external reference spectra (i.e., spectral signatures for the different soil types present) were not used for the analysis, the spectral values in the image were used to create a synthetic reference spectra by altering the threshold values for the analysis. The SID analysis for each image was performed using all six spectral bands and seven possible classifications. Threshold values were iteratively selected based on the histograms of the spectral end members and the classification results for each analysis. Previous studies have shown that SID analysis can be used to map materials present in a stream bed (Lecki et al. 2005) including water and vegetation. This study focused on classifying only the sediments that make up shoals in the river with the goal to monitor changes over time by filtering out the vegetation and the water.

To keep the results comparable between the K-Means clustering and the SID classification, the K-Means clustering analyses were performed with 7 clusters. All analysis was performed on the TOA Reflectance images. After the classifications were complete the results were filtered using the Normalized Difference Vegetation Index (*NDVI*), and the Normalized Difference Water Index (*NDWI*). The *NDVI* is a ratio between the reflectance in the red band and the *NIR* band (Kriegler et al. 1969) calculated using the following equation:

$$NDVI = \frac{NIR - RED}{NIR + RED}$$

where *NIR* is the TOA reflectance in the *NIR* band and *RED* is the TOA reflectance in the red band. Because plants reflect the majority of NIR light and absorb red light, the *NDVI* value for plants is typically high. In this analysis a value of 0.85 or higher was selected to represent plants, and pixels with an NDVI value of 0.85 or more were filtered out of the classification results and replaced with values of zero. Since the vegetation from the 2023 image is generally dead/browned for the winter, the 2023 image classifications were filtered using the 2022 NDVI results.

The *NDWI* is similar to the *NDVI* but uses the *NIR* band and the green band (Gao 1996), and is calculated using the following equation:

$$NDWI = \frac{GREEN - NIR}{GREEN + NIR}$$

where *GREEN* is the TOA reflectance in the green band. In this case the green band penetrates the water while the *NIR* band is reflected by the water. In the analysis, a value of 0.8 or higher was selected to represent water and any pixels with a *NDWI* value of 0.8 or more were filtered out of the classification results and replaced with values of zero. Due to changes in water levels each image was filtered with its own *NDWI* calculations.

The satellite image from January 2023 had full snow coverage for approximately 31% of the image in the area of the analysis. In the case of the SID analysis the variance between the snow pixel values and the soil values is relatively high, which has an effect on the classification of the

soils. For this reason, the snow pixels were masked to an average value of water in each individual band. This allowed the snow values to essentially be ignored by the SID analysis, and it also allowed the pixels to be masked out as water following the classification using the NDWI filtering. For consistency, snow filtering was applied to the images prior to K-Means clustering as well. It should be noted that only pixels that are completely covered in snow were filtered out. There are some cases where a "light dusting" of snow is present, but these pixels were not filtered out, which could also affect the classification. This was most prevalent on the downstream shoal.

RESULTS

Filtered SID results for both the 2022 and 2023 images are shown in Figure 2. In both cases, values and their corresponding classification group are as follows: 0.0 (Dark Blue) is the filtered area where values were removed, 0.1 (Blue) is a mixture of sand and gravel, 0.2 (Teal) is not present in the shoals, 0.3 (Green) is dark sand, 0.4 (Yellow) is not present in the shoals, 0.5 (Orange) is light sand, 0.6 (Red) is cobbles and gravels, and 0.7 (Maroon) is a mixture of gravel and sand.

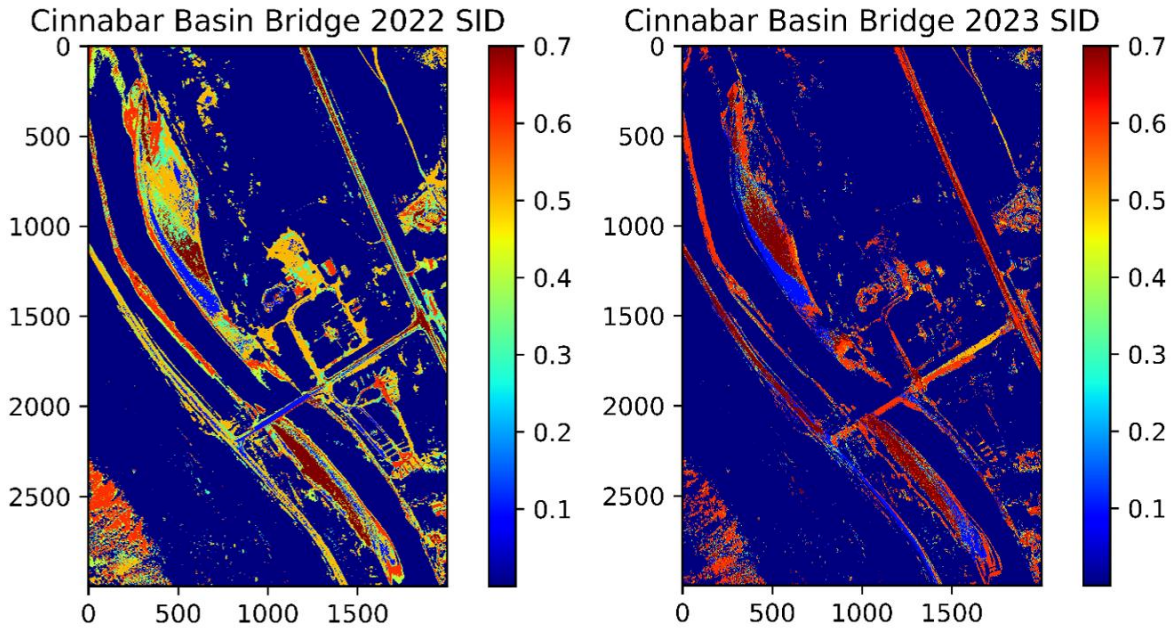

Figure 2. SID Results for 2022 image(left) and 2023 image (right). The classification values are as follows: 0.0 (Dark Blue) = filtered out, 0.1 (Blue) = sand and gravel 0.2 (Teal) = not represented in shoals, 0.3 (Green) =dark sand, 0.4 (Yellow) = not represented in shoals, 0.5 (Orange) = light sand, 0.6 (Red) = cobbles and gravel, 0.7 (Maroon) = gravel and sand

The classifications of the shoals were verified by observations and using site photos taken during the October 2022 field mission, the TrueColor pansharpened satellite images, and high resolution (approximately 3cm) drone photos taken during the field survey. The 2023 image generally shows less classification groups than the 2022 image, this is most apparent for the downstream shoal. Part of this can be explained by the snow coverage in the image. As seen in

Figure 1, most of the snow was accumulated on the sandy areas of the shoal, therefore removing the majority of the sand classifications from the image. Despite the snow filtering, there are still other areas of the shoals where the classification results are not as diverse as the 2022 image classification. It is hypothesized that the light dusting of snow present on some of the pixels from the 2023 image had a significant enough effect on the overall reflectance of the pixels that those pixels were classified as a separate, more homogeneous, material with less overall variability.

Filtered K-Means clustering results are shown in Figure 3. The color values for the K-Means clustering were modified to match the SID results as closely as possible, however not all values could be matched exactly. The K-Means classifications groups are as follows: 0.0 (Dark Blue) is the filtered area where values were removed, 0.1 (Blue) is sand, 0.2 (Teal) is medium dark sand, 0.3 (Green) is dark sand, 0.4 (Yellow) is not present in the shoals, 0.5 (Orange) is light sand, 0.6 (Red) is cobbles and gravels, and 0.7 (Maroon) is a mixture of sand and gravels.

The K-Means clustering analysis resulted in more classifications in the sandy areas and less classifications in the gravel and sand mixtures of the shoals. This likely occurred because the color of the sands varies more with moisture content than gravel and cobbles, and K-Means clustering is sensitive to any color variations, while SID is less sensitive to changes in reflection due to color in the same material (albedo).

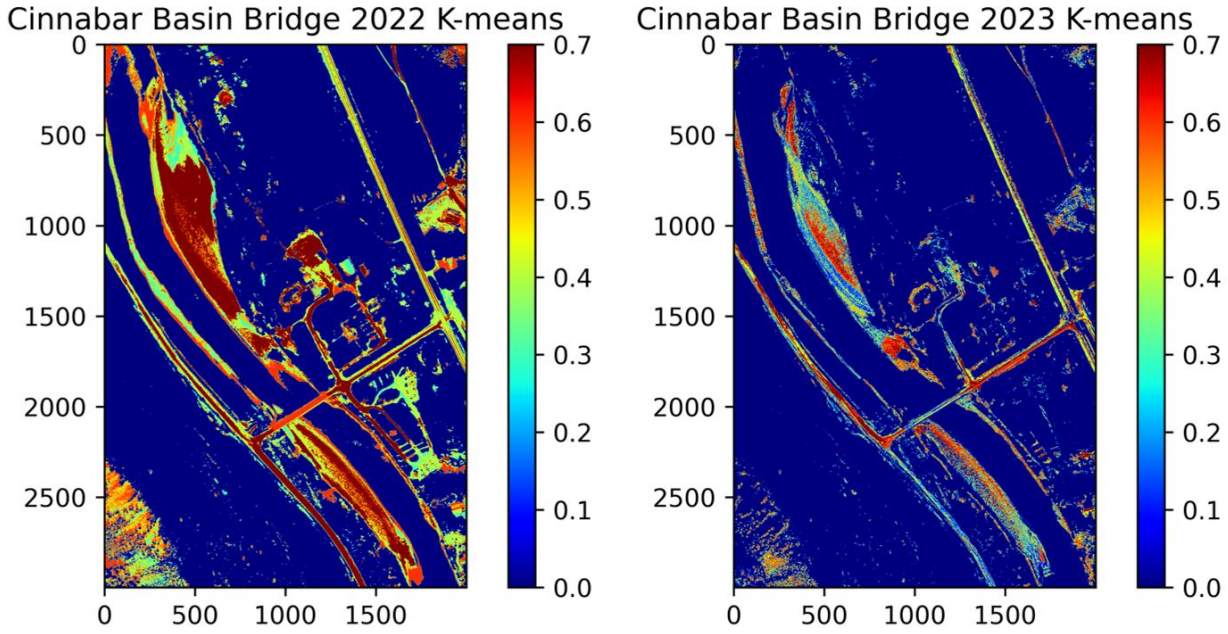

Figure 3. K-Means Clustering results for 2022 image (left) and 2023 image (right). Classifications groups are as follows: 0.0 (Dark Blue) = filtered area where values were removed, 0.1 (Blue) = sand, 0.2 (Teal) = medium dark sand, 0.3 (Green) = dark sand, 0.4 (Yellow) is not present in the shoals, 0.5 (Orange) = light sand, 0.6 (Red) = cobbles and gravels, and 0.7 (Maroon) = a mixture of sand and gravels.

The K-Means clustering results show more classifications in the gravel and cobble areas when the NDVI, and NDVI filtering were performed on the image before the K-Means clustering was performed. An example image where the K-Means clustering was performed after the filtering of the 2022 image is shown in Figure 4.

The classifications are as follows: 0.0 (Dark Blue) is the filtered area where values were removed, 0.1 (Blue) is gravel and sand, 0.2 (Teal) not present in the shoals, 0.3 (Green) is dark sand, 0.4 (Yellow) is not present in the shoals, 0.5 (Orange) is not present in the shoals, 0.6 (Red) is cobbles and gravels, and 0.7 (Maroon) is a mixture of sand and gravels. The increase in classifications in this case is likely caused by a general decrease in variance between the pixels since all vegetation and water values were removed. This allowed for closer classification in the shoals themselves.

Overall, both the SID analysis and K-means clustering classifications provide sediment classifications that generally match the observations made on site, the high-resolution drone images, and the pansharped RGB TrueColor images. The SID analysis in particular was able to produce sediment classifications in zones that match on site observations and are consistent across the downstream and upstream shoals. An example site photo of the upstream shoal is shown in Figure 5 for comparison.

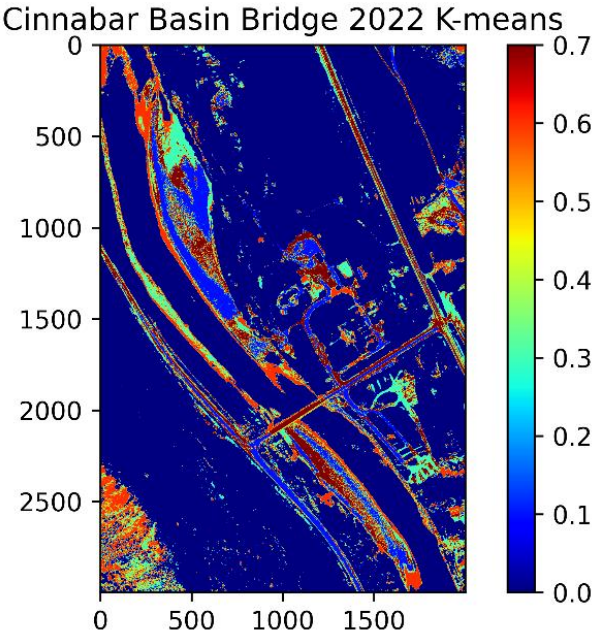

Figure 4. K-Means Clustering results for 2022 image filtered for NDVI and NDWI prior to K-Means Clustering analysis. Classifications groups are as follows: 0.0 (Dark Blue) is the filtered area where values were removed, 0.1 (Blue) is gravel and sand, 0.2 (Teal) not present in the shoals, 0.3 (Green) is dark sand, 0.4 (Yellow) is not present in the shoals, 0.5(Orange) is not present in the shoals, 0.6 (Red) is cobbles and gravels, and 0.7 (Maroon) is a mixture of sand and gravels.

The K-means clustering also provided reasonable results but is more susceptible to changes in moisture content of the sediments, particularly in sands where the color can change significantly with changes in moisture content. The presence of a light dusting of snow in the 2023 images affected the results and both the SID analysis and the K-means clustering showed less classification groups in the shoals due to the snow cover. Unless snow is a constant in the images the results may suggest that performing the classifications with snow present should be avoided.

Figure 5. Photo of the upstream shoal, looking upstream. From right to left the sediment generally changes from sand, gravel and sand, to gravel and cobbles, generally matching the results of the classifications.

CONCLUSION

Two methods for classifying sediment types in sand and gravel shoals from high resolution satellite images were tested. Results show that SID analysis from very high resolution (30cm at nadir) pansharpened images can provide soil classification maps for shoals in rivers. K-Means clustering can also provide classification maps; however, the results may differ from the results of the SID analysis and are susceptible to soil moisture content, and the multispectral band selected for the analysis. The classifications maps provided by these methods could be used to track the changes in shoals over time and determine how they can affect surrounding infrastructure. In this case, the presence of snow in the image from 2023 had a negative effect on the classification maps, and a direct comparison between the maps generated from the 2022 images and the 2023 images was not possible. The snow also tended to accumulate on the shore of the shoals which prevented comparison of the classification of the soils uncovered in the 2023 image by the lower water level.

ACKOWLEDGEMENTS

The authors acknowledge funding from the Office of Naval Research (ONR) through grant N00014-23-S-B001, from the National Science Foundation through grant CMMI-1822307, and from the GEER Association supported by the National Science Foundation through grant CMMI- 1826118. The authors would also like to thank Dennis McIntosh (Yellowstone Forever Association) who assisted the team during the field mission.

REFERENCES

Baodong, M., Lixin, W., and Shanjun, L. (2008). Remote Sensing Detection for Subsidence-Resulted Water Body and Solid-Waste Dump in Coal Mine : Yanzhou Being a Case. *The International Archives of the Photogrammetry, Remote Sensing and Spatial Information Sciences – Volume XXXVII Part B6b*.

ERDAS. *ERDAS Fiels Guide*, 5th ed., ERDAS Inc., Atlanda, GA, USA, 1999.
FHWA. (2005). Field Observations and Evaluations of Streambed Scour at Bridges. U.S Department of Transportation, FHWA-RD-03-052.
Gao, B. C. (1996). NDWI—A normalized difference water index for remote sensing of vegetation liquid water from space. *Remote Sensing of Environment*, 58(3), 257–266.
Hartigan, J. A., and Wong, M. A. (1979). Algorithm AS 136: A K-Means Clustering Algorithm. *Applied Statistics*, 28(1).
Kriegler, F. J., Malila, W. A., Nalepka, R. F., and Richardson, W. (1969). Preprocessing transformations and their effects on multispectral recognition. *Proceedings of the 6th International Symposium on Remote Sensing of Environment*.
Leckie, D. G., Cloney, E., Jay, C., and Paradine, D. (2005). Automated mapping of stream features with high-resolution multispectral imagery: An example of the capabilities. In *Photogrammetric Engineering and Remote Sensing* (Vol. 71, Issue 2).
Pléiades Imagery User Guide, Airbus, Munich, Germany, 2021.
Smith, S., Holland, D. A., and Longley, P. A. (n.d.). (2004). *The Importance of Understanding Error in LIDAR Digital Elevation Models*.
Sumer, B. M., and Fredsøe, J. (2002). "Scour Around a Single SlenderPile", *The Mechanics of Scour in the Marine Environment*. World Scientific: River Edge, NJ.